

## Effect of temperature on the fracture toughness of anisotropic shale and other rocks

MICHAEL R. CHANDLER<sup>1,2\*</sup>, PHILIP G. MEREDITH<sup>1</sup>, NICOLAS BRANTUT<sup>1</sup> & BRIAN R. CRAWFORD<sup>3</sup>

<sup>1</sup>*Rock and Ice Physics Laboratory, Department of Earth Sciences, University College London, UK*

<sup>2</sup>*Present address: School of Earth, Atmospheric and Environmental Sciences, The University of Manchester, UK*

<sup>3</sup>*ExxonMobil URC, Houston, TX, USA*

\*Correspondence: [mike.chandler@manchester.ac.uk](mailto:mike.chandler@manchester.ac.uk)

**Abstract:** Fracture toughness was measured for a range of rock materials as a function of temperature between ambient temperature and 150°C. Measurements were made along all three principal crack orientations for the transversely isotropic Mancos shale and in single orientations for the more isotropic Darley Dale sandstone, Indiana limestone and Lanhehin granite. Fracture toughness was measured using a modified short-rod method with the sample and loading equipment enclosed within an elevated temperature chamber. A slight increase in  $K_{Ic}$  was observed in Lanhehin granite with increasing temperatures up to 54°C, before a steady decrease at higher temperatures. For the sandstone and limestone, little change was observed in  $K_{Ic}$  over the studied temperature range. In measurements on Mancos shale at elevated temperatures, fracture toughness was seen to increase slightly with increasing temperature in the arrester orientation over this range, while remaining constant in the other two orientations. These observations can be explained in terms of the development of thermally induced microfractures parallel to the bedding planes in this material. A bimodal distribution of  $K_{Ic}$  values in the short-transverse orientation was not observed, as it has been for previously published measurements at ambient conditions.



**Gold Open Access:** This article is published under the terms of the CC-BY 3.0 license.

The hydraulic fracturing of gas shales has led to renewed interest in their mechanical and microstructural properties. Fracture toughness is an important mechanical property influencing the propagation of hydraulic fractures. It represents the critical value of the stress intensity for a material, above which a fracture will propagate dynamically.

The fracture toughness,  $K_{Ic}$ , and ductility corrected fracture toughness,  $K_{Ic}^c$ , were measured on rock samples at temperatures from ambient to 150°C using the method described by Chandler *et al.* (2016), which is a modification of the standard short-rod methodology described by ISRM (1988). The temperature range chosen roughly corresponds to that likely to be encountered in the uppermost 5 km of the crust, close to the maximum depth where the hydraulic fracturing of shales is utilized. Experiments were conducted in all three principal crack orientations (Fig. 1) on samples of the anisotropic Mancos shale and in single orientations on samples of the more isotropic Darley Dale sandstone, Indiana limestone and Lanhehin granite.

Two distinct effects potentially need to be accounted for when recording fracture toughness at elevated temperatures: (1) changes in the microstructural state of samples due to the differential expansion of adjacent mineral grains – this is caused by thermal expansion anisotropy within single mineral phases, differences in the thermal expansion coefficients between different mineral phases and, often, both of these effects (Meredith & Atkinson 1985); and (2) changes in the fracture propagation process at the crack tip due to the increased temperature.

Here, the subject of the investigation was the effect of temperature on the fracture process at the crack tip, so it was important to ensure that the materials were in the same micromechanical state at the start of testing at each test temperature. Therefore, to remove the effects of material changes, the samples were heat-treated to the maximum test temperature (150°C) prior to all experimental measurements. This procedure aimed to ensure that any thermal cracking caused by the heating would be the same in each sample and hence the

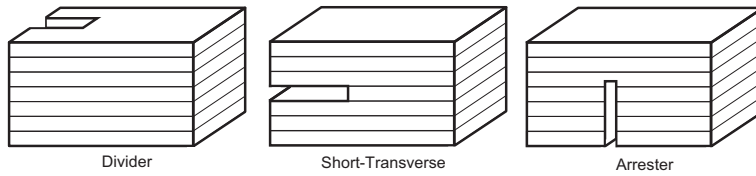


**Fig. 1.** The three principal crack plane orientations relative to the bedding (anisotropy) plane: divider, short-transverse and arrestor. Figure modified after Chong *et al.* (1987) and Chandler *et al.* (2016).

micromechanical state would be the same regardless of the test temperature. The evolution of the recorded fracture toughness with temperature should therefore represent the true evolution of the fracture process. Acoustic emissions were recorded during the heat treatment and the acoustic emission output was uniform over the whole temperature range, with no observed peak in acoustic emission activity. This suggests that thermal microcracking does indeed occur over this temperature range in these materials, supporting the idea that a pre-heating treatment of samples is necessary.

### Test materials

A full description of the petrographic, elastic and mechanical properties of the Mancos shale is provided in Chandler *et al.* (2016) and thus only a summary description is provided here. Mancos shale is a Late Cretaceous shale deposited 90–70 Ma ago in the Rocky Mountain area of western Colorado and eastern Utah. It provides the source for many of the shale plays in the Rockies (Longman & Koepsell 2005). Figures 2 and 3 show a photograph and a magnified scanning electron microscopy (SEM) image, respectively, of the layered structure of the Mancos shale. The layering within the material is

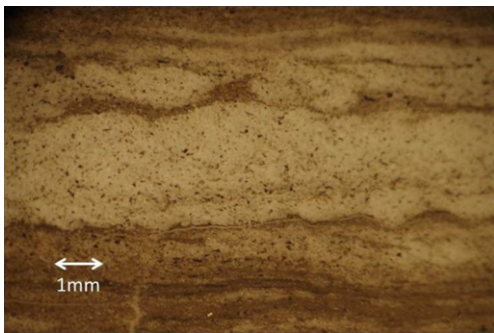


**Fig. 2.** Optical microscopy image of layering in the Mancos shale. Interbedded layers of fine-grained clay (dark) and coarser layers of siltstone (light) are observed to undulate. Figure reproduced from Chandler *et al.* (2016).

visible from the micrometre to centimetre scale. The dark brown and dark grey layers in Figures 2 and 3, respectively, consist of a fine-grained clay matrix containing elongate fragments of organic matter. The light brown and light grey layers in the same figures consist of terrigenous sand and silt containing calcite cement. The thinly laminated structure is shown in Figure 3 and is as expected for these outcrop samples because it suggests that they are not deep-sourced (Loucks *et al.* 2012). McLennan *et al.* (1983) used X-ray diffraction analysis to study samples of Mancos shale and found 25–100% quartz and 10–30% dolomite, with <15% calcite, illite, kaolinite, chlorite, feldspar, pyrite and apatite. These components agree broadly with the mineralogical interpretation of the SEM elemental analysis conducted by King (2013).

Darley Dale sandstone is a feldspathic sandstone from Derbyshire, UK with a porosity of *c.* 14% and no notable layering (Heap *et al.* 2009). It is commonly used in rock mechanics because it provides repeatable experimental results. Indiana limestone is a beige, medium-grained fossiliferous limestone

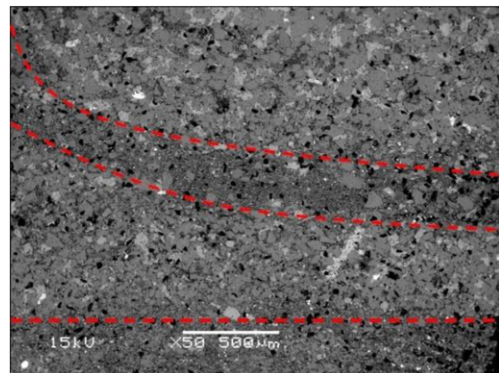


**Fig. 3.** SEM image showing layering within the Mancos shale. Layer boundaries are indicated by dashed red lines. Narrow layers of fine-grained clay (dark) are interwoven with bands of silt (light) containing calcite, dolomite, feldspar and quartz grains. Black spots of organic material are visible within both layer types. Figure reproduced from Chandler *et al.* (2016) and King (2013).

## EFFECT OF TEMPERATURE ON FRACTURE TOUGHNESS

composed chiefly of calcium carbonate. It is very homogeneous with a porosity of 10–15% (Schmidt & Huddle 1977). The Lanhelin granite is a coarse-grained, blue–grey granodiorite from Brittany, France. It has a porosity of *c.* 1% and a grain size of *c.* 2 mm (Griffiths *et al.* 2015).

### Methodology

Elevated temperature experiments were conducted using the same equipment and modified short-rod methodology as used under ambient conditions by Chandler *et al.* (2016), with the following exceptions.

The entire loading train shown in Figure 4 (see also fig. 8 in Chandler *et al.* 2016) was enclosed within an Instron 3119–007 (–150 to +350°C) environmental chamber. Solartron Metrology OP/1.5/G displacement transducers with a temperature capability of up to 150°C were used to record the crack mouth opening displacement (CMOD).

A short-rod sample consists of a 60 mm diameter cylinder with a chevron notch cut parallel to its axis to leave a triangular ligament of intact material. A tensile load is then applied from the sample end in a direction perpendicular to the plane of the

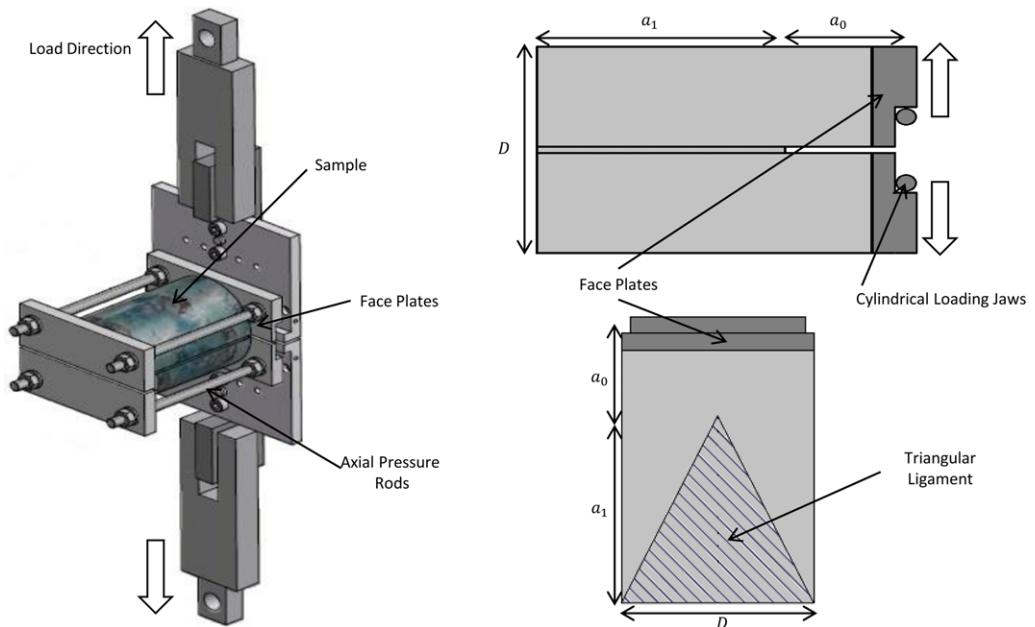
ligament (Fig. 4). This causes a crack to propagate along the ligament from the tip of the chevron. The level I fracture toughness is then calculated from the peak load,  $F_{\max}$ , using

$$K_{Ic} = \frac{A_{\min} F_{\max}}{D^{1.5}} \quad (1)$$

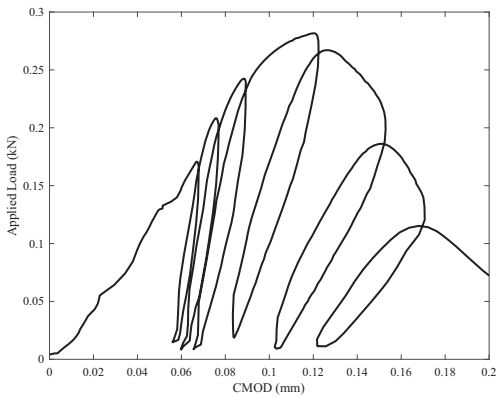
where  $A_{\min}$  is a dimensionless constant found to be equal to 24.0 by Ouchterlony (1989). The level II fracture toughness is then found by applying a correction based on the cyclic loading curves following the ISRM (1988) method.

Figure 5 shows an example of a load v. CMOD curve from an experiment conducted at 118°C on Indiana limestone. As in Chandler *et al.* (2016), the peak load from the level II cyclic loading tests was used to determine  $K_{Ic}$  and the cyclic loading correction was applied to determine  $K_{Ic}^c$ .

Prior to testing, all samples were heat-treated to a temperature of 150°C and held at this temperature for 60 min before being cooled to ambient conditions. The samples were then reheated to the desired experimental temperature at a rate of 1°C/min and held at this temperature for a further 60 min to equilibrate before the start of the test. This heating rate is



**Fig. 4.** Experimental setup used for the short-rod fracture toughness experiments. The bottom jaw is fixed in place and the upper jaw is raised to apply the tensile load. Both jaws are free to rotate to maintain the correct alignment. Two LVDT displacement transducers are mounted on the rear of the jaws to measure the crack mouth opening displacement and are also used to control the displacement rate. The face plates are seen on the front of the sample, abutting the jaws. The axial pressure modification is seen in the studding connecting the face plates and rear plates. Image and design by N. Hughes. Figure reproduced from Chandler *et al.* (2016)



**Fig. 5.** Example load v. crack mouth opening displacement (CMOD) record from an experiment conducted on Indiana limestone at 118°C.  $K_{Ic}$  is calculated from the peak load using equation (1).  $K_{Ic}^c$  is calculated by multiplying  $K_{Ic}$  by  $m$ , which is a ductility correction factor calculated from the hysteresis during cyclic loading. The reloading cycles become progressively less steep, representing inelastic deformation within the material (Chandler *et al.* 2016).

low enough for the thermal gradient across the sample to be relatively insignificant (*c.* 3°C). To test the need for this pre-heating treatment of the samples, a second series of measurements were also conducted on non-heat-treated samples of Indiana limestone and Darley Dale sandstone for comparison.

## Results and discussion

Both  $K_{Ic}$  and  $K_{Ic}^c$  were measured as functions of temperature for Lanhelin granite, Darley Dale sandstone, Indiana limestone and Mancos shale. The results are given in Table 1.

Figure 6 shows the variation in  $K_{Ic}$  with increasing temperature for Lanhelin granite compared with values for other crystalline rocks: Icelandic basalt (Balme *et al.* 2004), Westerly granite and gabbro (Atkinson *et al.* 1984; Meredith & Atkinson 1985). All the rocks exhibited the same general trend of an initial increase followed by a gradual decrease in  $K_{Ic}$  with increasing temperature.

Meredith & Atkinson (1985) described this trend in terms of the development of thermal microcracks. Up to *c.* 100°C, a relatively small number of isolated microcracks develop. When the macrofracture tip encounters one of these microcracks oriented in a direction unfavourable to the propagation direction, it acts to blunt the macrofracture, so increasing the fracture resistance (seen as an increase in  $K_{Ic}$ ). Glover *et al.* (1995) observed a similar pattern and explained it as being due to the thermal expansion of crystallites closing up pre-existing

microfractures. At higher temperatures, it is argued that the microcrack density increases due to an increase in both the number of cracks and their length. This leads to crack interaction and coalescence, and hence weakening and a decrease in fracture resistance (Balme *et al.* 2004).

The magnitude of our Lanhelin granite results varies from those of the other researchers as a result of the microstructural and textural differences between the igneous rocks. However, the forms of the curves are remarkably consistent with the Westerly granite results of both Atkinson *et al.* (1984) and Meredith & Atkinson (1985), despite the experimental conditions for all three studies being very different. Westerly granite results of Atkinson *et al.* (1984) were for experiments conducted at ambient temperature on samples that had previously been heated to the desired temperature before being cooled. Therefore the measurement is of the effect on  $K_{Ic}$  of thermal microcracking to a range of specific temperatures. By contrast, Meredith & Atkinson (1985) conducted their experiments and measured  $K_{Ic}$  at elevated temperatures, but did not perform any thermal pre-treatment. Their measurements should therefore incorporate the combined effect of both the microstructural change due to thermal microcracking and the effect of temperature on the fracture process. For comparison, our experiments were also conducted at elevated temperatures, but on samples that had been thermally pre-treated to 150°C. Therefore our results should only incorporate the effect of temperature on the fracture process and should be independent of microstructural changes.

The data and their trends are remarkably similar even though they were obtained on two different materials using different experimental methodologies. If this trend occurred due solely to thermal microcrack development, then our results would not be expected to agree with those of Atkinson *et al.* (1984) and Meredith & Atkinson (1985). By contrast, if the trend occurred solely due to a temperature effect on the fracture propagation process, then the results of Atkinson *et al.* (1984) would not be expected to agree with the other two because their experiments were conducted on heat-treated samples, but at ambient temperature. These effects were discussed in depth by Balme *et al.* (2004) (their figure 7). It appears likely that the results of Atkinson *et al.* (1984) and Meredith & Atkinson (1985) demonstrate an initial temperature strengthening caused by crack-blunting as a result of microcrack formation. Our Lanhelin granite results and the results of Balme *et al.* (2004) also appear to feature an initial temperature strengthening, but caused by microcrack closure as a result of thermal expansion. This effect appears to be much stronger in the Icelandic basalt of Balme *et al.* (2004) than in the Lanhelin granite presented here. This may be due

## EFFECT OF TEMPERATURE ON FRACTURE TOUGHNESS

**Table 1.** Mean fracture toughness values for measurements at elevated temperatures. In each case, the uncertainty listed is the standard deviation over  $n$  experiments

Material	Orientation	Temperature (°C)	$K_{Ic}$ (MPa m <sup>1/2</sup> )	$K_{Ic}^c$ (MPa m <sup>1/2</sup> )	$m$	No. of experiments ( $n$ )
Lanhelin granite		22	1.52	1.87	1.23	1
Lanhelin granite		54	1.65	2.18	1.32	1
Lanhelin granite		86	1.58	2.13	1.35	1
Lanhelin granite		118	1.49	2.14	1.44	1
Lanhelin granite		150	1.39	1.78	1.29	1
Lanhelin granite		175	1.37*			1
Lanhelin granite		200	1.31*			1
Darley Dale sandstone	Arrester	22	0.70 ± 0.04	0.98 ± 0.08	1.39 ± 0.03	2
Darley Dale sandstone	Arrester	54	0.77 ± 0.04	1.19 ± 0.35	1.54 ± 0.37	2
Darley Dale sandstone	Arrester	86	0.78 ± 0.10	1.16 ± 0.12	1.50 ± 0.05	2
Darley Dale sandstone	Arrester	118	0.72 ± 0.15	1.12 <sup>†</sup>	1.36 <sup>†</sup>	2
Darley Dale sandstone	Arrester	150	0.72 ± 0.13	1.30 <sup>†</sup>	1.61 <sup>†</sup>	2
Indiana limestone	Arrester	22	0.36 ± 0.07	0.53 ± 0.12	1.48 ± 0.07	2
Indiana limestone	Arrester	54	0.37 ± 0.02	0.42 ± 0.08	1.30 ± 0.26	2
Indiana limestone	Arrester	86	0.34 ± 0.09	0.48 ± 0.06	1.17 ± 0.28	2
Indiana limestone	Arrester	118	0.39 ± 0.08	0.49 ± 0.00	1.11 ± 0.17	2
Indiana limestone	Arrester	150	0.34 ± 0.10	0.51 ± 0.13	1.28 ± 0.25	2
Mancos shale	Divider	22	0.56 ± 0.18	1.06 ± 0.24	1.71 ± 0.06	3
Mancos shale	Divider	60	0.39 ± 0.10	0.49 ± 0.16	1.37 ± 0.16	2
Mancos shale	Divider	100	0.57 ± 0.10	0.97 ± 0.19	1.68 ± 0.05	2
Mancos shale	Divider	150	0.44 ± 0.03	0.74 ± 0.10	1.65 ± 0.05	2
Mancos shale	Short-Transverse	22	0.22 ± 0.12	0.49 ± 0.12	1.51 ± 0.04	2
Mancos shale	Short-Transverse	60	0.13 ± 0.07	0.22 ± 0.14	1.71 ± 0.06	2
Mancos shale	Short-Transverse	100	0.12 ± 0.08	0.20 ± 0.11	1.61 ± 0.17	2
Mancos shale	Short-Transverse	150	0.16 ± 0.06	0.32 <sup>†</sup>	1.48 <sup>†</sup>	2
Mancos shale	Arrester	22	0.49 ± 0.07	0.54 ± 0.16	1.34 ± 0.41	3
Mancos shale	Arrester	60	0.41 ± 0.07	0.53 ± 0.09	1.30 ± 0.02	2
Mancos shale	Arrester	100	0.71 ± 0.04	1.01 ± 0.07	1.45 ± 0.05	2
Mancos shale	Arrester	150	0.67 ± 0.12	0.81 ± 0.13	1.65 ± 0.05	2

\*Denotes measurements at temperatures above that used for heat treatment (150°C). These samples are expected to have undergone additional thermal microcracking.

<sup>†</sup>Denotes that the LVDTs failed during one of these experiments, so that  $K_{Ic}$  is the mean of two measurements, but  $K_{Ic}^c$  and  $m$  are determined from one measurement only.

to the much smaller grain size of the basalt, allowing more effective microcrack closure. The temperature weakening at higher temperatures in each case is expected to be due to increasing microcrack connectivity.

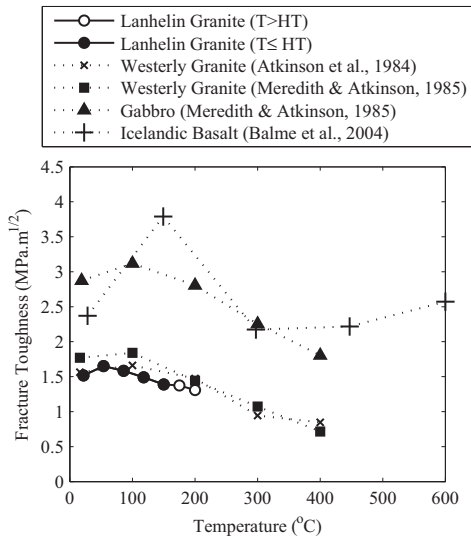
Figure 7 shows the variation of the ductility corrected fracture toughness ( $K_{Ic}^c$ ) with temperature for Darley Dale sandstone and Indiana limestone for both heat-treated and non-heat-treated samples. The data for the non-heat-treated samples are listed in Table 2. In general, the same approximate trend is observed for the non-heat-treated samples as for the heat-treated samples and the measurements largely lie within experimental uncertainty. As expected, the heat-treated and non-heat-treated measurements at 150°C agree well for both materials.

Figure 8 compares our data for non-heat-treated Darley Dale sandstone and Indiana limestone with previously published fracture toughness data for sedimentary rocks (Kimachi sandstone, Tage tuff and Khuff limestone) conducted on non-heat-treated samples at elevated temperatures (Al-Shayea *et al.*

2000; Funatsu *et al.* 2004). Our  $K_{Ic}$  values were plotted rather than  $K_{Ic}^c$  here for direct comparison with Al-Shayea *et al.* (2000) and Funatsu *et al.* (2004) and also so that our values for  $T > 150^\circ\text{C}$  could be included.

All of the materials appear to display a slight increase in  $K_{Ic}$  with increasing temperature for temperatures  $c. > 120^\circ\text{C}$ . Funatsu *et al.* (2004) explain this increase in  $K_{Ic}$  above 120°C as being due to the dehydration of clay minerals within their sedimentary material. As the clay minerals dehydrate, the coefficient of friction between platelets increases and the material therefore strengthens. However, little temperature dependence of  $K_{Ic}$  was observed at lower temperatures, except for the Khuff limestone, which displayed increasing  $K_{Ic}$  values with increasing temperature at all temperatures tested by Funatsu *et al.* (2004).

Fracture toughness experiments were conducted on heat-treated samples of Mancos shale in all three principal crack orientations (as described in Chandler *et al.* 2016) at 22, 60, 100 and 150°C. Two



**Fig. 6.** Variation of  $K_{Ic}$  with temperature for a range of igneous rocks. Westerly granite results are reproduced from Atkinson *et al.* (1984) and Meredith & Atkinson (1985). The gabbro results are the mean of the two blocks tested by Meredith & Atkinson (1985). The Icelandic basalt results are from Balme *et al.* (2004). For the Lanhelin granite in this study, the closed circles represent experiments conducted below the heat treatment temperature and the open circles represent experiments conducted above this temperature.

experiments and measurements of  $K_{Ic}$  and  $K_{Ic}^c$  were made at each temperature for each orientation. The mean values at each temperature are plotted in Figure 9 with their associated standard deviations. At 22°C, the values all lay within the

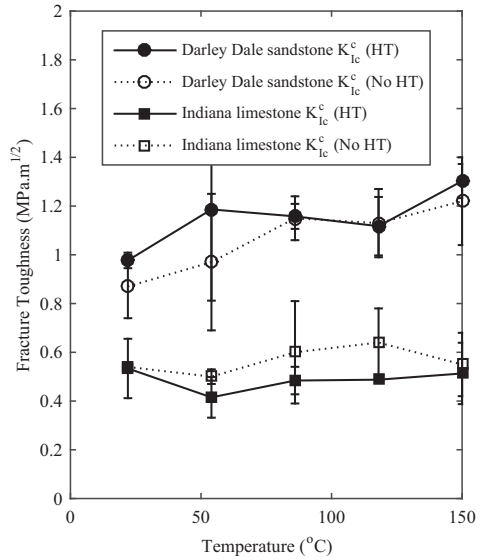


**Fig. 7.** Variation of  $K_{Ic}^c$  with temperature for samples of Darley Dale sandstone and Indiana limestone, with and without heat treatment. The differences with heat treatment largely lie within experimental uncertainties.

experimental uncertainty of those listed by Chandler *et al.* (2016). The same anisotropy was observed with  $K_{Ic}$  in the arrester and divider orientations being similar, whereas the short-transverse orientation display a lower  $K_{Ic}$ . This initial anisotropy was believed to relate to the bedding planes in the material.

In the divider orientation,  $K_{Ic}$  and  $K_{Ic}^c$  were each seen to fall at 54°C, but were otherwise not seen to vary significantly over the temperature range

**Table 2.** Mean fracture toughness values measured on non-heat-treated samples at elevated temperatures. Measurements at temperatures > 150°C have no associated  $K_{Ic}^c$  or  $m$  values, as these temperatures lie outside the operational range of the LVDTs. In each case, the uncertainty listed is the standard deviation over  $n$  experiments

Material	Orientation	Temperature (°C)	$K_{Ic}$ (MPa m <sup>1/2</sup> )	$K_{Ic}^c$ (MPa m <sup>1/2</sup> )	$m$	No of experiments (n)
Darley Dale sandstone	Arrester	22	0.63 ± 0.06	0.87 ± 0.13	1.38 ± 0.13	2
Darley Dale sandstone	Arrester	54	0.68 ± 0.04	0.97 ± 0.28	1.42 ± 0.20	2
Darley Dale sandstone	Arrester	86	0.75 ± 0.01	1.15 ± 0.09	1.55 ± 0.06	2
Darley Dale sandstone	Arrester	118	0.80 ± 0.12	1.13 ± 0.14	1.42 ± 0.11	2
Darley Dale sandstone	Arrester	150	0.75 ± 0.13	1.22 ± 0.18	1.64 ± 0.18	2
Darley Dale sandstone	Arrester	175	0.82	—	—	1
Darley Dale sandstone	Arrester	200	0.80	—	—	1
Indiana limestone	Arrester	22	0.48 ± 0.05	0.54 ± 0.01	1.14 ± 0.09	2
Indiana limestone	Arrester	54	0.41 ± 0.01	0.50 ± 0.03	1.22 ± 0.03	2
Indiana limestone	Arrester	86	0.38 ± 0.11	0.60 ± 0.21	1.59 ± 0.10	2
Indiana limestone	Arrester	118	0.34 ± 0.02	0.64 ± 0.14	1.84 ± 0.28	2
Indiana limestone	Arrester	150	0.32 ± 0.03	0.55 ± 0.13	1.71 ± 0.24	2
Indiana limestone	Arrester	175	0.38	—	—	1
Indiana limestone	Arrester	200	0.44	—	—	1

## EFFECT OF TEMPERATURE ON FRACTURE TOUGHNESS

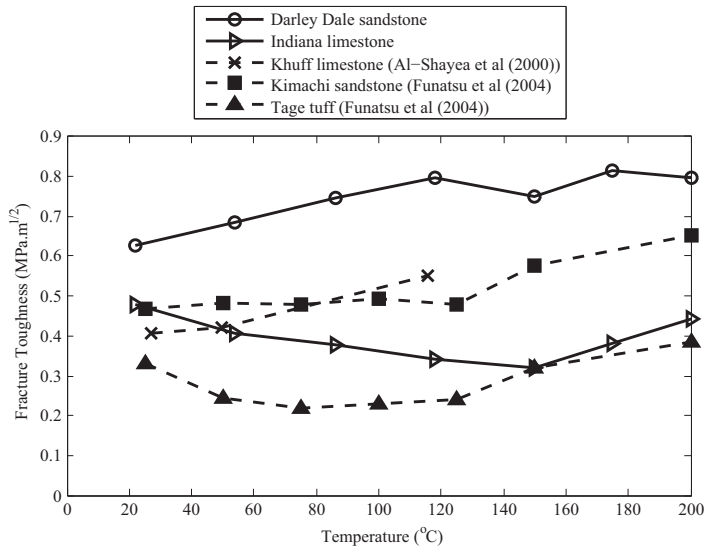


**Fig. 8.** Variation of  $K_{Ic}$  with temperature for a range of non-heat-treated sedimentary materials. Kimachi sandstone and Tage tuff values are reproduced from Funatsu *et al.* (2004). Khuff limestone results are reproduced from Al-Shayea *et al.* (2000).

tested from 22 to 150°C. In the short-transverse orientation, neither  $K_{Ic}^c$  or  $K_{Ic}^d$  changed significantly between 22 and 150°C. Notably the values measured were much closer to the lower of the two values recorded at ambient temperature by Chandler *et al.* (2016) in this orientation. At no time during the elevated temperature measurements was a value close to the higher of the ambient temperature values recorded. In the arrester orientation,  $K_{Ic}^c$ ,  $m$  and  $K_{Ic}^d$  all increased slightly between 22 and 150°C, but only within the temperature interval 60–100°C was this increase larger than the uncertainty in the measurement.

Nadeau & Reynolds (1981) showed that the major clay components of the Mancos shale are illite and smectite. Mikhail & Guindy (1971) showed that illite and smectite begin to dehydrate at around 70 and 120°C, respectively. Therefore, if the clay dehydration effect described by Funatsu *et al.* (2004) is occurring in the shale, temperature strengthening of  $K_{Ic}^c$  would be expected above these temperatures. In both the divider and arrester orientations, a small increase in  $K_{Ic}^c$  was observed at temperatures >60°C, but in each case this change lay well within the experimental variability.

The disappearance of the higher of the two ambient short-transverse orientation values might suggest that the heat treatment induced the growth of microfractures parallel to the bedding, thus allowing the main fracture to tunnel from the stronger beds into the weaker beds. In addition, the slight increase in the arrester orientation  $K_{Ic}^c$  value with

temperature might suggest that the microfractures generated during heat treatment of the shale material open up as the sample is heated and that these microfractures are preferentially oriented parallel to the bedding planes. Microfractures lying perpendicular to the main fracture would impede a fracture propagating in the arrester orientation by acting to blunt the main fracture, so that a larger stress intensity would be required to overcome this barrier (Meredith & Atkinson 1985). This effect has been observed in Kimmeridge shale over the temperature range 0–200°C by Figueroa-Pilz *et al.* (2017) using X-ray tomography.

Pyrak-Nolte *et al.* (1990) noted that perpendicularly oriented fractures should be expected to impede the propagation of P waves, but that fractures oriented parallel to the propagation direction should not significantly affect the P wave velocity ( $v_p$ ). Therefore, to test this hypothesis, the samples on which  $v_p$  had been measured as a function of angle from bedding-parallel by Chandler *et al.* (2016) were heat-treated to 150°C.  $v_p$  was then measured again as a function of angle from bedding-parallel and the results are shown in Figure 10. In the bedding-parallel direction, a decrease of only 0.6% in  $v_p$  was observed following heat treatment. By contrast, a much larger decrease of 3.1% in  $v_p$  was observed in the bedding-perpendicular direction after heat treatment. This suggests that the majority of microfractures formed during the heat treatment lie in a bedding-parallel orientation, which supports the hypothesis described here.

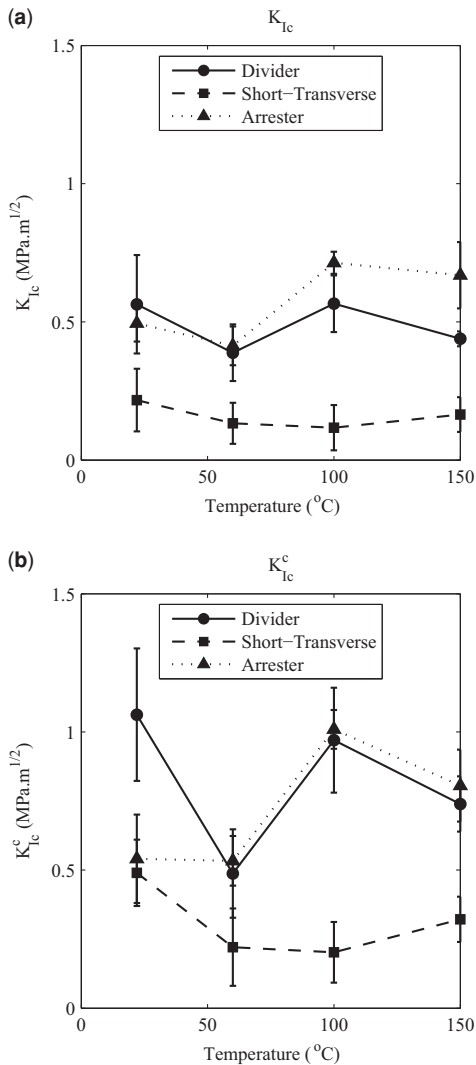


**Fig. 9.** (a) Variation of  $K_{Ic}$  with temperature for the three principal crack orientations in the Mancos shale. (b) Variation of  $K_{Ic}^c$  with temperature for the three principal crack orientations in the Mancos shale. Each point shows the mean of  $n$  experiments from Table 1.

## Conclusions

The results presented here suggest that, in sedimentary rocks, the fracture toughness changes only very little as a function of temperature over the range 0–120°C. A modest increase was observed at temperatures between 120 and 200°C, which Funatsu *et al.* (2004) explained as being due to an increase in platelet friction as clay minerals dehydrate. This finding is in agreement with Paterson & Wong

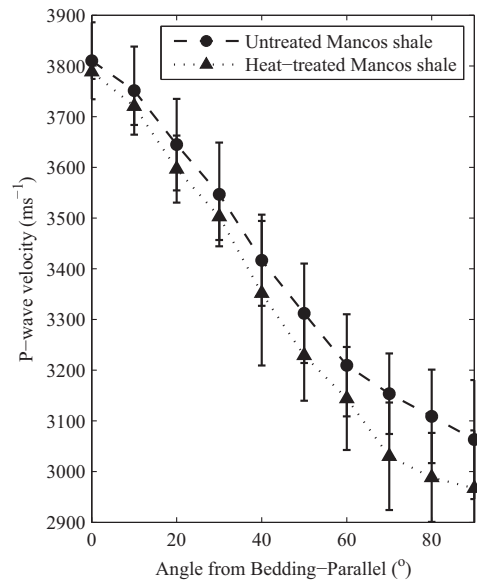


**Fig. 10.** Variation of ultrasonic P wave velocity ( $v_p$ ) with angle from bedding-parallel through dry cores of Mancos shale before and after heat treatment. The untreated data are reproduced from Chandler *et al.* (2016). In the bedding-parallel direction, a 0.6% decrease in  $v_p$  was observed with heat treatment. In the bedding-perpendicular direction, a larger 3.1% decrease in  $v_p$  was observed after heat treatment.

(2005), who concluded that brittle fracture displays a relatively small temperature dependence until such a temperature is reached that the fracture mechanism can change. This insensitivity to temperature has been observed in brittle fracture experiments with the exception of time-dependent, subcritical crack growth in the presence of water. In that specific case, the temperature sensitivity is higher because the chemical behaviour of water is highly dependent on temperature (Brantut *et al.* 2013). The experiments described here were conducted on dry samples and produced dynamic fractures, so the low temperature sensitivity is in agreement with previously published work.

In the Mancos shale specifically, fracture toughness was not observed to vary significantly over this temperature range. Heat treatment does appear to suppress the higher of the two short-transverse toughness values recorded by Chandler *et al.* (2016), which may be due to the formation of thermal microfractures parallel to the bedding planes. Because the temperature sensitivity of  $K_{Ic}$  was seen to be low, and the anisotropy observed at ambient conditions remained, hydraulic fracturing studies are likely to be best served by assuming that the sensitivity to temperature will be small

## EFFECT OF TEMPERATURE ON FRACTURE TOUGHNESS

compared with the effect of elevated confining pressure at depth.

This work was supported by ExxonMobil URC and a UCL Impact Scholarship award. MC and NB acknowledge support from the Natural Environment Research Council (grants NE/M001458/1 and NE/K009656/1, respectively). Thanks are given to Neil Hughes, John Bowles, Steve Boon and Jim Davy for their work on developing the experimental methodology used here.

## References

- AL-SHAYEA, N., KHAN, K. & ABDULJAUWAD, S. 2000. Effects of confining pressure and temperature on mixed-mode (I-II) fracture toughness of a limestone rock. *International Journal of Rock Mechanics and Mining Sciences*, **37**, 629–643, [https://doi.org/10.1016/S1365-1609\(00\)00003-4](https://doi.org/10.1016/S1365-1609(00)00003-4), <http://www.science-direct.com/science/article/pii/S1365160900000034>
- ATKINSON, B., MACDONALD, D. & MEREDITH, P. 1984. Acoustic response and fracture mechanics of granite subjected to thermal and stress cycling experiments. In: CLAUSTHAL, W. (ed.) *Proceedings of the 3rd International Conference on Crack Growth. Technical Report in Geological Structures and Materials*. Trans-Tech, Zurich, 5–18.
- BALME, M., ROCCHI, V., JONES, C., SAMMONDS, P., MEREDITH, P. & BOON, S. 2004. Fracture toughness measurements on igneous rocks using a high-pressure, high-temperature rock fracture mechanics cell. *Journal of Volcanology and Geothermal Research*, **132**, 159–172, [https://doi.org/10.1016/S0377-0273\(03\)00343-3](https://doi.org/10.1016/S0377-0273(03)00343-3)
- BRANTUT, N., HEAP, M., MEREDITH, P. & BAUD, P. 2013. Time-dependent cracking and brittle creep in crustal rocks: a review. *Journal of Structural Geology*, **52**, 17–43, <https://doi.org/10.1016/j.jsg.2013.03.007>
- CHANDLER, M.R., MEREDITH, P.G., BRANTUT, N. & CRAWFORD, B.R. 2016. Fracture toughness anisotropy in shale. *Journal of Geophysical Research: Solid Earth*, **121**, 1706–1729, <https://doi.org/10.1002/2015JB012756>
- CHONG, K.P., KURUPPU, M.D. & KUSZMAUL, J.S. 1987. Fracture toughness determination of layered materials. *Engineering Fracture Mechanics*, **28**, 43–54, [https://doi.org/10.1016/0013-7944\(87\)90118-4](https://doi.org/10.1016/0013-7944(87)90118-4)
- FIGUEROA-PILZ, F., DOWEY, P. ET AL. 2017. Synchrotron tomographic quantification of strain and fracture during simulated thermal maturation of an organic-rich shale, UK Kimmeridge Clay. *Journal of Geophysical Research – Solid Earth*, <https://doi.org/10.1002/2016JB013874>
- FUNATSU, T., SETO, M., SHIMADA, H., MATSUI, K. & KURUPPU, M. 2004. Combined effects of increasing temperature and confining pressure on the fracture toughness of clay bearing rocks. *International Journal of Rock Mechanics and Mining Sciences*, **41**, 927–938, <https://doi.org/10.1016/j.ijrmms.2004.02.008>
- GLOVER, P.W.J., BAUD, P. ET AL. 1995.  $\alpha/\beta$  phase transition in quartz monitored using acoustic emissions. *Geophysical Journal International*, **120**, 775–782, <https://doi.org/10.1111/j.1365-246X.1995.tb01852.x>
- GRIFFITHS, L., HEAP, M., REUSCHLÉ, T., BAUD, P. & SCHMITTBUHL, J. 2015. Permeability enhancement by shock cooling. *EGU General Assembly, 12–17 April, 2015, Vienna, Austria*. id.5183 <http://meetingorganizer.copernicus.org/EGU2015/EGU2015-5183-1.pdf>
- HEAP, M.J., BAUD, P., MEREDITH, P.G., BELL, A.F. & MAIN, I.G. 2009. Time-dependent brittle creep in Darley Dale sandstone. *Journal of Geophysical Research: Solid Earth*, **114**, b07203, <https://doi.org/10.1029/2008JB006212>
- ISRM 1988. Suggested methods for determining the fracture toughness of rock. *International Journal of Rock Mechanics and Mining Science & Geomechanics Abstracts*, **25**, 71–96.
- KING, F. 2013. *An investigation into the porosity of the Mancos Shale*. Master's thesis, University College London.
- LONGMAN, M. & KOEPEL, R. 2005. *Defining and Characterizing Mesaverde and Mancos Sandstone Reservoirs Based on Interpretation of Formation Microimager (FMI) Logs, Eastern Uinta Basin, Utah*. Utah Geological Survey, Salt Lake City.
- LOUCKS, R., REED, R., RUPPEL, S. & JARVIE, D. 2012. Morphology, genesis, and distribution of nanometer-scale pores in siliceous mudstones of the Mississippian Barnett Shale. *Journal of Sedimentary Research*, **79**, 848–861.
- MCLENNAN, J., ROEGIERS, J. & MARX, W. 1983. The Mancos Formation: an evaluation of the interaction of geological conditions, treatment characteristics and production. In: MCLENNAN, R.M. (ed.) *Low Permeability Gas Reservoirs Symposium*. SPE/DOE, Denver, CO, 63–69.
- MEREDITH, P. & ATKINSON, B. 1985. Fracture toughness and subcritical crack growth during high-temperature tensile deformation of westerly granite and black gabbro. *Physics of the Earth and Planetary Interiors*, **39**, 33–51, [https://doi.org/10.1016/0031-9201\(85\)90113-X](https://doi.org/10.1016/0031-9201(85)90113-X)
- MIKHAIL, R. & GUINDY, N.M. 1971. Rates of low-temperature dehydration of montmorillonite and illite. *Journal of Applied Chemistry and Biotechnology*, **21**, 113–116, <https://doi.org/10.1002/jctb.5020210407>
- NADEAU, P. & REYNOLDS, R. 1981. Burial and contact metamorphism in the Mancos Shale. *Clay and Clay Minerals*, **29**, 249–259.
- OUCHTERLONY, F. 1989. On the background to the formulae and accuracy of rock fracture toughness measurements using ISRM standard core specimens. *International Journal of Rock Mechanics and Mining Sciences & Geomechanics Abstracts*, **26**, 13–23, [https://doi.org/10.1016/0148-9062\(89\)90521-4](https://doi.org/10.1016/0148-9062(89)90521-4)
- PATERSON, M.S. & WONG, T.F. 2005. *Experimental Rock Deformation – The Brittle Field*. Springer, Berlin.
- PYRAK-NOLTE, L.J., MYER, L.R. & COOK, N.G.W. 1990. Anisotropy in seismic velocities and amplitudes from multiple parallel fractures. *Journal of Geophysical Research: Solid Earth*, **95**(B7), **11345–11358**, <https://doi.org/10.1029/JB095iB07p11345>
- SCHMIDT, R. & HUDDLE, C. 1977. Effect of confining pressure on fracture toughness of indiana limestone. *International Journal of Rock Mechanics and Mining Sciences & Geomechanics Abstracts*, **14**, 289–293, [https://doi.org/10.1016/0148-9062\(77\)90740-9](https://doi.org/10.1016/0148-9062(77)90740-9)